ACCURATE TRANSMISSION LINE CHARACTERIZATION ON HIGH AND LOW-RESISTIVITY SUBSTRATES

Geert Carchon[+], Walter De Raedt[*], Bart Nauwelaers[+]

[+] K.U.Leuven, div. ESAT-TELEMIC, Kasteelpark Arenberg 10, B-3001 Heverlee, Belgium
* IMEC, div. MCP-HDIP, Kapeldreef 75, B-3001 Heverlee, Belgium
E-mail: carchon@imec.be; Tel: ++32/(0)16/288191; Fax: ++32/(0)16/281501

***Abstract* — Differences in probe-tip-to-line geometry and substrate permittivity between measurement and calibration wafer deteriorate measurement accuracy. This is especially the case when measurements are performed on lossy Silicon substrates. Two novel general techniques are presented which characterise the discontinuities near the probe-tip based on the measurement of two lines with different length. The equivalent elements representing the discontinuity are extracted at each frequency point together with the propagation constant and the characteristic impedance of the line. The obtained results are superior to previous methods with a reduced number of measurements. The validity of the method is demonstrated with measurements of CPW-lines on low and high resistivity Silicon and GaAs.**

I. INTRODUCTION

Probe-tip discontinuities have a large effect on the extracted lineparameters of measured lines. Especially the characteristic impedance (Z_c) is very sensitive. This has been reported for measurements on high [1, 2] and low-resistivity [3, 4] substrates. They are present when an off-wafer calibration is used, however, also in on-wafer calibrations, the width and slot of the measured lines usually differs from the calibration structures. A technique is therefore needed to accurately characterize Z_c and the propagation constant (γ) of the measured lines. The technique should be generally applicable to both high as low-resistivity substrates and should have the ability to accurately characterize the probe-tip discontinuities and remove their effect from the measurements.

In [1] the calibration comparison method is presented: a 2^{nd}-tier M-TRL calibration is performed to obtain the error boxes relating a second calibration (using transmission lines with unknown Z_c) to a previous reference calibration. The error boxes contain the S-parameters of the discontinuities followed by an ideal transformer translating the reference impedance to the Z_c of the measured lines. The Z_c is estimated from this errorbox in different ways:

- in [5], the extracted Z_c is insensitive to reference plane transformations but is sensitive to a parasitic admittance at the probe-tip, hereby degrading the accuracy.
- an improved interpretation of the error-boxes [3], makes the method insensitive to the presence of a shunt admittance. However, this technique is sensitive to reference plane transformations and does not account for the presence of a series inductance due to the step-in-width between the probe and strip or a probe misalignment.

Both methods require a correct choice of sign to determine Z_c and its value should, thus, be approximately known. This is especially difficult when the Z_c of the measured lines approaches 50Ω, e.g., if $|\Gamma| = 0.01$, the obtained value is either 49Ω or 51Ω.

[4] uses the contact-pad model we have already suggested in [2, 6] but requires more measurements than the presented methods.

II. PROPOSED ERROR-BOX CALCULATION

A typical two-port measurement is given in Fig. 1: the DUT is embedded in the probe-tip-to-line transitions, represented by R_A and R_B. As the discontinuities on both sides are equal, the measurement problem can be assumed to be symmetrical, such that only R_A is to be determined.

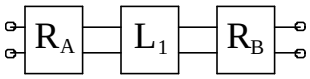

Fig. 1: Typical two-port measurement problem: the line L_1 is embedded in R_A and R_B representing the discontinuities.

After an initial (reference) calibration on the calibration substrate, a thru and line are measured on the measurement substrate. This provides γ, S_{11A} and $X=(S_{12A}.S_{21A})/S_{22A}$ [7]. For a reciprocal model, $S_{12A}=S_{21A}$ and an additional relation is given by equation (1) with S_{11L_1} the measured S_{11} and l_1 the length of the shortest line [7]. The extracted S_{21A} is given by equation (2). The choice of sign is made by demanding $\angle S_{21A} \approx 0$ (the differences between measurement and calibration wafer are small): the solutions are centred round 0°, 90°, 180° and 270°.

γ is accurately extracted over the entire frequency range, but, just as in a TRL-calibration, the method for the determination of the error-boxes becomes unstable near $\Delta l=180°$ [7]. To prevent the need for a third line, the extracted values can be easily interpolated from nearby

frequencies as the extracted parasitics are nearly constant as a function of frequency. It should be mentioned that [3, 5] solves this problem by measuring multiple line-pairs.

$$S_{22A}^2 = e^{2gl_1}\left(1+\frac{X}{S_{11L_1}-S_{11A}}\right)^{-1} \quad (1)$$

$$S_{21A} = e^{jkp/2}\cdot\sqrt[4]{X^2 e^{2gl_1}\left(1+\frac{X}{S_{11L_1}-S_{11A}}\right)^{-1}} \quad \text{k=0...3} \quad (2)$$

II. Error-Box Models and Calculation

The measured lines usually do not have the same contact geometry as the calibration standards and also the substrate may differ. This leads to a different behaviour of the shunt stub underneath the probe-tip and a step-in-width between probe and strip. The location of the probe-tips is also not known exactly. The methods should, therefore, be able to accurately compensate for an arbitrarily large shunt admittance at the probe-tip, some extra inductance due to the step-in-width and a reference plane transformation due to the not precisely known location of the probe-tips.

The proposed models are given in Fig. 2

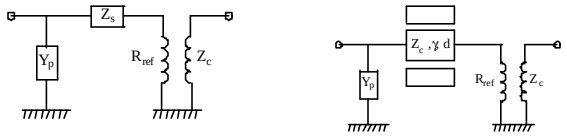

Fig. 2: Proposed error-models: method-1 (left), method-2 (right).

A. Method-1

The first method is insensitive to an arbitrary series impedance (Z_s) and shunt admittance (Y_p) at the probe-tip. The proposed model for the error-box is shown in Fig. 2 (left). Z_s and Y_p can take any arbitrary form but for simplicity, Z_s can be regarded as a series inductance (L_S) and resistance (R_S), while Y_p can be regarded as a parallel conductance (G_g) and capacitance (C_g). Losses due to a different contact geometry are represented by R_S and G_g, differences in contact geometry and substrate permittivity by L_S and C_g (e.g. the difference in open-end effect of the shunt stub underneath the probe-tip or the step-in-width between probe-tip and strip). Small errors in the probe position are accounted for by C_g and L_S.

The ABCD-representation of the extracted S-parameters should satisfy equation (3) with R_{ref} the reference impedance of the system after the initial calibration, usually 50 Ω.

$$\begin{bmatrix} 1/n_A & n_A.Z_S \\ Y_p/n_A & n_A.[1+Z_S Y_p] \end{bmatrix} \text{ with } n_A = \sqrt{R_{ref}/Z_c} \quad (3)$$

$$\text{and } Z_S = R_S + jwL_S \text{ and } Y_p = G_g + jwC_g$$

From equation (3), the Z_c and probe-tip parasitics are readily obtained. No choice of sign has to be made for the determination of Z_c as opposed to [3, 5].

B. Method-2

The second method is insensitive to an arbitrary shunt admittance (Y_p) at the probe tips and to an arbitrary shift in the location of the reference plane. It, therefore, combines the advantages from [5] and [3]. The proposed error-box model is shown in Fig. 2 (right), d is the length of the line.

The ABCD-matrix of the error-box should satisfy equation (4). The location of the reference plane can be found from equation (5) as γ is already known. Z_c and Y_p can be calculated from equation (6) and equation (7). Again, no choice of sign is required for the determination of Z_c as opposed to [3, 5].

$$\begin{bmatrix} \cosh(x)/n_A & n_A.Z_c.\sinh(x) \\ \dfrac{Y_p\cosh(x)}{n_A}+\dfrac{\sinh(x)}{n_A.Z_c} & n_A.[Y_p Z_c\sinh(x)+\cosh(x)] \end{bmatrix} \quad (4)$$

$$\text{with } x = g.d\ ;\ Y_p = G_g + jwC_g\ ;\ n_A = \sqrt{R_{ref}/Z_c}$$

$$g.d = B/(R_{ref}A) \quad (5)$$

$$Z_c = (R_{ref}A^2)/(\cosh^2(g.d)) \quad (6)$$

$$Y_p = (n_A C)/(\cosh(g.d)) - \tanh(g.d)/Z_c \quad (7)$$

IV. Measurements on GaAs

To demonstrate the methods, measurements were performed using Cascade wafer probes (pitch 100µm) and an HP8510 network analyzer. The system was calibrated with TRL, using the LRM ISS G-S-G Alumina substrate of Cascade Microtech (ε_r=9.9, w=50 µm, s=25 µm). The reference plane was set to 25 µm beyond the physical beginning of the line by positioning with contact marks. Several lines (lengths 250µm and 3200µm) with different contact geometries were measured on GaAs. The contact geometries of the lines and the results obtained by implementing method-1 and method-2 are summarized in TABLE 1.

A. Extracted Parasitics

The methods were first implemented on the calibration substrate: since all parasitics are removed during calibration, the obtained values are a measure for the accuracy of the method. From the values in TABLE 1, we conclude that the obtained accuracy is very good for both methods.

The extracted C_g for the different lines using method-1 are given in Fig. 3: they are approximately constant over the whole frequency band. The extracted L_S, R_S and G_g (method-1) for the 50 Ω line are given in Fig. 4: L_S only varies slightly as a function of frequency, R_S and G_g are negligible. The value of the extracted L_S for the other lines is given in TABLE 1.

TABLE 1: Contact geometries of the tested lines together with the extracted parasitics.

		line 1	line 2	line 3	line 4	ISS
	$Z_{c,\,MDS}$	30 Ω	40 Ω	50 Ω	70 Ω	50 Ω
	W_{line}	80 µm	60 µm	30 µm	17 µm	50 µm
	W_{slot}	10 µm	20 µm	22.5 µm	40 µm	25 µm
Method 1	Z_c	29.4 Ω	39 Ω	48 Ω	65.5 Ω	50 Ω
	C_g	5.9 fF	4 fF	2.5 fF	1 fF	0.1 fF
	L_s	1 pH	1 pH	1.4 pH	2 pH	0.4 pH
Method 2	Z_c	29.4 Ω	39 Ω	48 Ω	65.5 Ω	50 Ω
	C_g	3.5 fF	3.9 fF	2.5 fF	0.7 fF	-0.2 fF
	d	7 µm	1 µm	1.5 µm	2.5 µm	1.2 µm

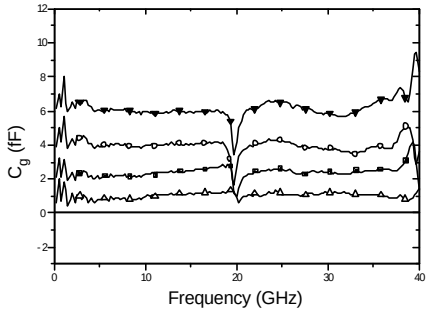

Fig. 3: Extracted C_g for a 70 Ω (-Δ-), a 50 Ω (-■-), a 40 Ω (-o-) and a 30 Ω (-▼-) line using method-1.

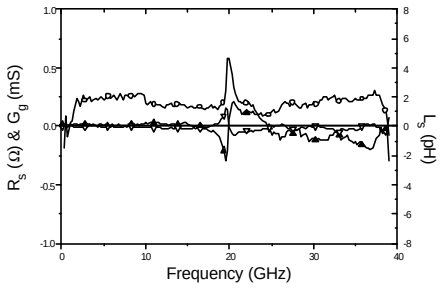

Fig. 4: Extracted L_s (-o-), R_s (-▲-) and G_g (-∇-) for the 50 Ω line using method-1.

The extracted d and C_g for the 50 Ω line using method-2, are given in Fig. 5: they are approximately constant over the whole frequency band. The other values are given in TABLE 1. Notice that an excellent probe-positioning has been obtained.

B. Extracted Line Parameters

The extracted Z_c for the 30 Ω-line using method-1 is given in Fig. 6 together with the extracted Z_c if no compensation is made. Our method gives a much smoother result due to the better removal of the parasitics. The extracted Z_c using method-1 and method-2 nearly coincide with a maximum difference of 4mΩ for the 50 Ω line over the 45 MHz-40 GHz band. As compared to method-1 [3] gives a maximum difference of 10 mΩ, while [1] results in a maximum difference of 0.5 Ω @ 40 GHz. This illustrates that, even for high-resistivity substrates, the presented techniques provide a higher accuracy and provide more insight in the parasitics which is advantageous to correctly interpret the obtained results.

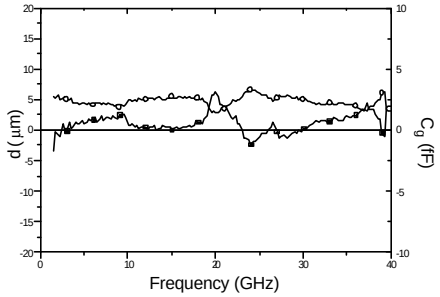

Fig. 5: Extracted d (reference plane transition) (-■-) and C_g (-o-) using method-2 for the 50 Ω line.

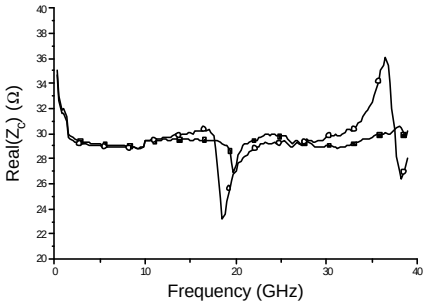

Fig. 6: The extracted Z_c using method-1 (-■-) is compared with the extracted Z_c if no compensation is made (-o-).

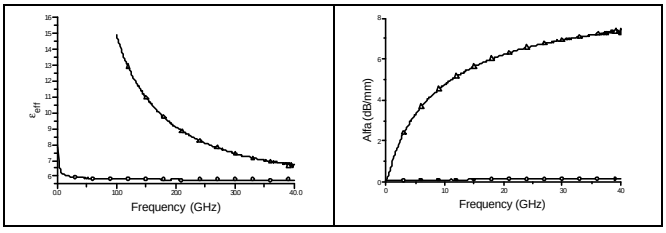

Fig. 7: The extracted ε_{eff} (left) and intrinsic losses (right) for the CPW-line on high (-o-) and low (-Δ-) resistivity silicon.

V. MEASUREMENTS ON SILICON

The methods have also been applied to low- and high-resistivity silicon with 3µm Cu-metallization. CPW lines (w=47µm, s=35µm) with lengths 510µm and 4510µm were characterized. The extracted ε_{eff} and α (dB/mm) are given in Fig. 7. The extracted Z_c using method-1 are given in Fig. 8. If uncompesated measurements were used, an error of +/-10% would be made on ε_{eff}@20GHz while the losses would be wrong by 5%. The accuracy of the 4 methods are compared in Fig. 9 and Fig. 10. Here the relative differences in the real and imaginary part of the extracted Z_c are given.

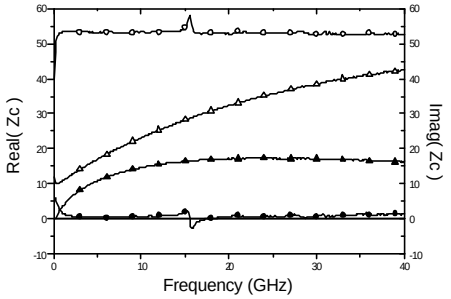

Fig. 8: The extracted Zc for the CPW-line on high and low resistivity silicon using method-1: real-part (-o-) and imaginary part (-●-) for the high-resistivity silicon line; real-part (-Δ-) and imaginary (-▲-) part for the low-resistivity silicon line.

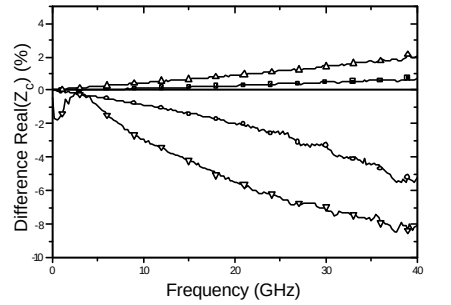

Fig. 9: Relative difference for real(Z_c) using the different methods (compared with method-1): (-■-) method-2, (-o-) method of [1], (-Δ-) method of [3], (-∇-) uncompensated measurements.

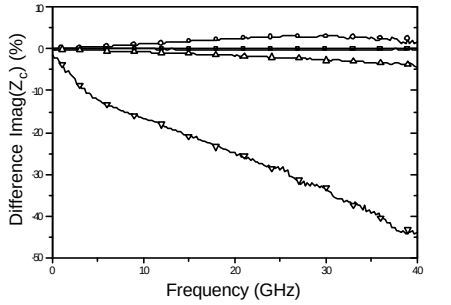

Fig. 10: Relative difference for imag(Zc) using the different methods (compared with method-1): (-■-) method-2, (-o-) method of [1], (-Δ-) method of [3], (-∇-) uncompensated measurements.

Method-1 and method-2 give nearly the same result (a maximum difference of +0.5% on the real-part, the difference on the imaginary part remains below 0.4%). As compared to method-1, [1] gives a maximum difference of –6% on the real part and +3% on the imaginary part, [3] a difference of +2% on the real part and –4% on the imaginary part. The uncompensated measurements (using [8]) result in a maximum difference of –9% on the real part and -45% on the imaginary part. We can conclude that our methods provide a higher accuracy than previous methods and that compensation for the probe-tip parasitics is required. The obtained I_s and d were nearly frequency independent, whereas C_g is frequency dependant.

VI. Discussion and Conclusions

Two novel general techniques have been presented which characterise the discontinuities near the probe-tip based on the measurement of 2 lines with different length. The equivalent elements of the discontinuity model are extracted at each frequency point together with γ and Z_c of the line. The results are superior to previous methods. The validity of the method is demonstrated with measurements of CPW-lines on GaAs, low and high resistivity silicon.

Both methods are insensitive to an arbitrary large admittance at the probetip. In addition, one method is insensitive to an arbitrary series impedance, the other is insensitive to an arbitrary shift in the location of the reference plane.

The presented techniques, therefore, require less measurements than [3-5] but with increased performance.

Acknowledgement

This work was supported by a scholarship granted by the Flemish Institute for the Advancement of SCientific-Technological Research in Industry (IWT).

References

[1] D. F. Williams and R. B. Marks, "Accurate transmission line characterization," *IEEE Microwave and Guided Wave Letters*, vol. 3, pp. 247-249, 1993.

[2] G. Carchon, B. Nauwelaers, W. De Raedt, D. Schreurs, and S. Vandenberghe, "Characterizing differences between measurement and calibration wafer in probe-tip calibrations," *Electronics Letters*, vol. 35, pp. 1087-1088, 1999.

[3] D. F. Williams, "Accurate characteristic impedance measurement on Silicon," *IEEE MTT-S*, pp. 1917-1920, 1998.

[4] A. Bracale, D. Pasquet, J. L. Gautier, N. Fel, V. Ferlet, and J. L. Pelloie, "A new method for characteristic impedance determination on lossy substrate," *IEEE MTT-S*, pp. 1481-1484, 2000.

[5] D. F. Williams, R. B. Marks, and A. Davidson, "Comparison of on-wafer calibrations," *ARFTG*, pp. 68-81, 1991.

[6] G. Carchon, D. Schreurs, S. Vandenberghe, B. Nauwelaers, and W. De Raedt, "Compensating differences between measurement and calibration wafer in probe-tip calibrations- de-embedding of line parameters," *EuMC*, pp. 259-264, 1998.

[7] R. R. Pantoja, M. J. Howes, J. R. Richardson, and R. D. Pollard, "Improved calibration and measurement of the scattering parameters of microwave integrated circuits," *IEEE Trans. on MTT*, vol. 37, pp. 1675-1680, 1989.

[8] Y. C. Shih, "Broadband characterization of conductor-backed coplanar waveguide using accurate on-wafer measurement techniques," *Microwave Journal*, pp. 95-105, 1991.